Journal of Applied Polymer Science

WILEY

Applied Polymer SCIENCE

RESEARCH ARTICLE OPEN ACCESS

The Mechanical Behavior of Dual TPU/Nylon 3D Printed Parts

Liam O'Connor

Materials and Structures (MAST) Research Group School of Physics, Engineering & Computer Science, Centre for Engineering Research, University of Hertfordshire, Hatfield, UK

Correspondence: Liam O'Connor (l.oconnor3@herts.ac.uk)

Received: 28 October 2025 | **Revised:** 20 January 2026 | **Accepted:** 23 January 2026

Keywords: applications | dual-material printing | elastomers | fused filament fabrication (FFF) | manufacturing | multi-material additive manufacturing | polyamide (nylon) | thermoplastic polyurethane (TPU)

ABSTRACT

This study examines how material arrangement and infill geometry affect the mechanical performance of dual-material fused-filament fabrication (FFF) parts made from thermoplastic polyurethane (TPU) and polyamide (Nylon). The goal was to identify printing strategies that balance strength, stiffness, and ductility for engineering applications. Specimens were printed in three configurations—Nylon-outer with TPU core, alternating TPU–Nylon layers, and TPU-outer with Nylon core—each using line, grid, and triangular infills. Tensile and flexural tests were conducted. Material arrangement was the dominant factor influencing performance. The Nylon-outer structure achieved the highest tensile (~13.4 MPa) and flexural (~74 MPa) strengths but showed low elongation (~12%–27%). The TPU-outer design improved ductility (up to ~34%) but reduced strength, while alternating TPU–Nylon layers provided a balanced response, combining high strength with ~30% elongation. Infill geometry further affected properties: line infill aligned with the load path enhanced both strength and ductility, whereas grid and triangular infills reduced performance. Nylon outer structures suit stiffness-critical components, TPU outer designs are ideal for flexible or damping parts, and alternating layers offer the best strength–ductility compromise. These insights clarify how dual-material FFF parameters can be tuned to meet specific mechanical requirements in engineered components.

1 | Introduction

Additive manufacturing has advanced from single-material printing to multi-material fused filament fabrication (FFF), where two or more polymers are combined in a single build [1–3]. This approach overcomes the limitations of individual polymers by embedding complementary properties in different regions of a part [4, 5]. A rigid thermoplastic can provide structural strength, while an elastomer adds compliance and energy absorption.

Such hybrid behavior is valuable across many industries. In automotive, components like vibration mounts, flexible housings, and crash-absorbing panels can benefit from combined stiffness and damping [6]. In aerospace, lightweight parts that must resist loads but also absorb vibration, such as interior panels or brackets, are well-suited to rigid–flexible designs [7]. In biomedical devices, orthopedic implants with a rigid shell and compliant core better replicate bone–cartilage interfaces and show improved integration [8]. Even in general engineering, structural components with built-in energy dissipation, such as tooling, fixtures, or consumer products, can be realized without assembly. Multi-material printing enables such systems to emerge fully formed from the printer, thereby reducing weight, cost, and part count.

Among candidate pairs, thermoplastic polyurethane (TPU) and polyamide (Nylon) are particularly promising [9]. TPU is a flexible elastomer with high elasticity, abrasion resistance, and the ability to dissipate energy [10]. Nylon is a semi-crystalline thermoplastic valued for tensile strength, stiffness, and durability,

This is an open access article under the terms of the Creative Commons Attribution License, which permits use, distribution and reproduction in any medium, provided the original work is properly cited.

© 2026 The Author(s). *Journal of Applied Polymer Science* published by Wiley Periodicals LLC.

though it requires careful processing [11]. Combining the two offers a balance of toughness and strength that is difficult to achieve with either alone. B. J. Rashmi et al. [9] reported that TPU–Nylon blends show higher modulus and yield strength than pure TPU while retaining elongation at break, confirming their complementary nature. In such hybrids, Nylon enhances stiffness and strength, while TPU contributes ductility and toughness.

Rigid–flexible laminates also illustrate this synergy. Acrylonitrile butadiene styrene (ABS)–TPU sandwich structures demonstrate a trade-off between strength and ductility. S. Kumar et al. [4] found that ABS–TPU–ABS specimens had higher flexural strength, while TPU–ABS–TPU configurations showed a 187% increase in bending elongation. This outcome matches the classic composite theory: the stiff outer layers carry bending loads, while the compliant layers allow deformation before failure. E. Brancewicz-Steinmetz et al. [12] similarly noted that stiff polylactic acid (PLA) ensures load absorption, while TPU layers limit crack propagation. Together, these studies show that dual-material prints can achieve both higher strength than elastomers and greater ductility than rigid plastics. Yet, most work has focused on PLA–TPU or ABS–TPU, leaving TPU–Nylon hybrids largely unexplored.

Another gap concerns infill geometry. Multi-material prints are typically produced with solid or simple raster infill, even though infill design strongly affects mechanical performance in single-material prints. Certain patterns, such as honeycomb, maximize tensile properties, while others, such as triangular grids, perform better in compression. J. Song et al. [13] showed that infill choice significantly alters strength and stiffness in mono-material systems; S. Turaka et al. [14] found that a rectangular infill outperformed honeycomb for ABS. However, similar studies for multi-material FFF are lacking. The interaction between material placement and complex infill designs can strongly influence load transfer and failure, yet this remains under-examined.

This study addresses these gaps by systematically evaluating the tensile and flexural properties of TPU–Nylon dual-material specimens. Different layer arrangements and infill patterns are compared to reveal how stiffness, strength, and ductility can be tuned through design. The findings provide guidelines for creating hybrid components that are strong, resilient, and well-suited to automotive, aerospace, and other load-bearing applications.

2 | Methodology

2.1 | Materials and Manufacturing

2.1.1 | Materials

Two commercially available thermoplastic filaments were used to fabricate dual-material test specimens: Thermoplastic Polyurethane (TPU) and Polyamide (Nylon). These materials were selected due to their contrasting mechanical characteristics, offering the potential for complementary performance in hybrid structures.

Ultimaker Black TPU 95A, supplied as 2.85 mm diameter filament. This elastomeric material has a high elongation at break and excellent abrasion resistance, making it suitable for flexible and impact-damping regions.

Ultimaker Transparent Nylon, supplied as 2.85 mm filament. Nylon is a semi-crystalline engineering polymer with high tensile strength, good interlayer adhesion, and chemical resistance, making it suitable for rigid load-bearing applications.

2.1.2 | Manufacturing

All specimens were fabricated using an Ultimaker S5 dual-extrusion fused filament fabrication (FFF) printer equipped with dual print cores and a heated build plate. This system enables reliable co-printing of flexible and rigid polymers, ensuring stable extrusion flow and consistent inter-material bonding.

The geometries were modeled in SolidWorks 2023 and exported as STL files. Slicing was performed in Ultimaker Cura 5.3, which allowed precise dual-material allocation and adjustment of processing parameters for both materials. Standard Cura profiles for TPU 95A and Nylon were used as the baseline and refined through preliminary print trials to achieve optimal interlayer adhesion and dimensional accuracy.

Three infill patterns—line, grid, and triangle—were used to assess the effect of internal structure on mechanical performance. All patterns were printed without layer-to-layer rotation, meaning the infill orientation in each layer was repeated identically through the part thickness. A rectilinear line pattern was applied, consisting of parallel filament strands printed in a single direction per layer. All infill lines were aligned parallel to the loading axis, providing continuous longitudinal channels and ensuring the filaments were loaded along their strongest direction. A 0°/90° crosshatch (grid) pattern was used, with two perpendicular filament sets deposited in each layer. One set of strands was aligned with the loading axis, and the other transverse to it. The intersecting lines formed a stacked square-lattice structure throughout the specimen. A triangular lattice was printed using three filament orientations (0°, +60°, −60°). One of the three directions was aligned with the loading axis, and the other two formed a 60° network. Repeating this pattern across layers produced continuous triangular cells throughout the part.

Given the high sensitivity of TPU and Nylon to extrusion temperature, bed temperature, and cooling conditions, the final printing parameters (Table 1) were determined based on both manufacturer guidelines and published literature. Prior studies have shown that TPU performs optimally around 220°C–240°C, with minimal cooling and moderate bed heating to enhance interlayer bonding while avoiding thermal degradation [15, 16]. Similarly, Nylon typically requires higher extrusion temperatures (240°C–260°C) and elevated bed temperatures (60°C–80°C) to improve crystallinity and minimize warping [17]. J. Slapnik et al. [18] further demonstrated that high extrusion temperatures and reduced cooling promote strong interfacial adhesion when combining TPU and Nylon in dual-material printing. Accordingly, the extrusion temperatures were set at 230°C for TPU and 250°C for Nylon to ensure reliable

co-extrusion and strong interlayer fusion. A bed temperature of 70°C was selected to maintain adhesion and limit warping across both materials. Cooling was minimized for Nylon (0%) to preserve bonding, while a low fan speed (20%) was applied for TPU to improve surface finish without compromising flexibility. The print speed (30–40 mm/s) and layer height (0.2 mm) were chosen following literature-reported optimal ranges for mechanical performance and dimensional accuracy.

TABLE 1 | Printing settings for both the TPU and Nylon filaments.

Parameter	TPU	Nylon
Nozzle temperature (°C)	230	250
Build plate temperature (°C)	70	70
Print speed (mm/s)	30	40
Cooling fan (%)	20	0
Layer height (mm)	0.2	0.2
Wall line count	3	3
Infill density (%)	95	95
Infill patterns	Line, Grid, Triangle	Line, Grid, Triangle

Two specimen geometries were fabricated:

- Dogbone-shaped tensile specimens (ASTM D638 Type V).
- Rectangular prism bending specimens (ASTM D790, three-point bending).

Specimens were printed upright, and the cross-sectional schematic shown in Figure 1 was used to maximize the effects of interlayer bonding and anisotropy. Each dogbone was printed without additional supports because the geometry permitted direct vertical printing. For bending specimens, three perimeter walls defined the outer shell; the remaining cross-sectional area was filled with the assigned infill pattern. For example, in a 10 mm-wide specimen, approximately 4 mm of the perimeter was solid material (2 mm on each side), whereas the central 6 mm contained infill. Representative photographs of the printed dogbone and flexural bar specimens are provided in Figure 2.

In terms of print quality, on one corner of the same samples, a protruding burr was visible in a circular shape, which

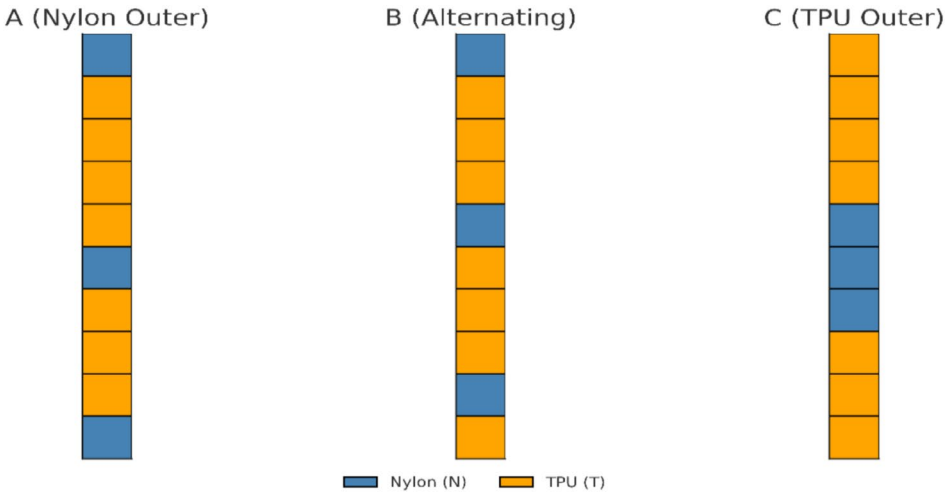

FIGURE 1 | Cross-section schematic of the layer set-up for all three configurations. [Color figure can be viewed at wileyonlinelibrary.com]

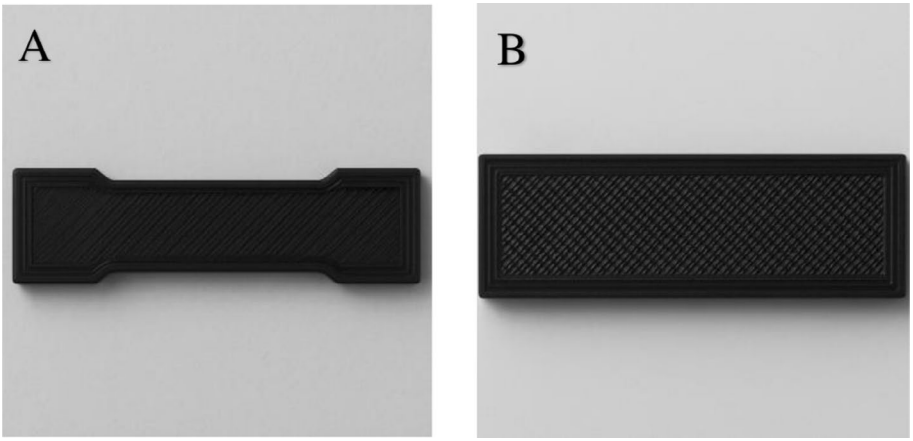

FIGURE 2 | Representative photograph of (A) tensile dogbone and (B) flexural bar.

extended across all layers. This is likely the corner at which the nozzle begins depositing filament on each iteration, leading to overextrusion and deformities. Figure 3A shows the extent of the burring, and Figure 3B shows the smaller burring (5 mm scale bar). It was observed that where nylon layers meet TPU layers, the nylon layers shift horizontally along the specimen length. Figure 3C shows the displacement of nylon, where the visible gap on the end edge is left (5 mm scale bar). This feature is exaggerated where there are two consecutive layers of nylon.

2.2 | Mechanical Testing

A total of 90 dual-material specimens were tested across three material configurations (A, B, C), each produced with line, grid, and triangle infill patterns. Only tensile and flexural tests were performed, as these loading modes are most sensitive to interfacial bonding, stiffness, and anisotropy in fused filament fabrication (FFF) structures. Similar testing strategies have been widely used in FFF research to evaluate layer adhesion and directional dependence in mechanical performance [19, 20].

2.2.1 | Tensile Testing

Tensile tests were performed following ASTM D638 Type V, which is widely adopted for polymer and additively manufactured materials [21]. Testing was conducted on an Instron 3369 Universal Testing Machine equipped with a 5 kN load cell at a crosshead speed of 5 mm/min, consistent with standard recommendations for plastic testing and with previous FFF studies [16, 19]. Due to the high flexibility of TPU and the difficulty of attaching an extensometer, strain was determined from crosshead displacement corrected for grip separation, following accepted practice for elastomeric and highly ductile polymers [21]. The extracted properties included Ultimate Tensile Strength (UTS), Young's Modulus, and Elongation at Break. Five replicates were tested for each configuration and infill pattern, with results reported as mean values and standard deviations used for error bars to ensure statistical reliability. This approach aligns with previous mechanical studies of FFF polymers that emphasize averaging over multiple specimens to capture inherent process variability [15, 20].

2.2.2 | Flexural Testing

Flexural performance was evaluated in accordance with ASTM D790, using a three-point bending fixture on the same Instron system. A 64 mm support span was employed, corresponding to approximately 16 times the specimen thickness, consistent with ASTM D790 recommendations [22, 23]. Tests were conducted at a crosshead speed of 2 mm/min under quasi-static loading; a rate commonly used for semi-rigid FFF polymers to capture accurate load–deflection behavior. From the resulting curves, Flexural Modulus and Flexural Strength were calculated using the standard equations defined in ASTM D790. Five replicates per configuration and infill pattern were tested to ensure statistical consistency. The use of flexural testing, alongside tensile testing, provides a comprehensive assessment of stiffness and interfacial bonding across tension–compression zones, consistent with the methodology adopted in recent multi-material FFF studies [19, 22].

3 | Results and Discussion

To evaluate how material arrangement and infill geometry influence tensile performance, we measured the ultimate tensile strength (UTS), Young's modulus, and elongation at break of the TPU–Nylon specimens. Figures 4–6 present these results for all configurations (A: Nylon outer shell, B: alternating Nylon/TPU layers, C: TPU outer shell) and infill patterns (Line, Grid, Triangle). Each data point is the average of multiple specimens, with error bars indicating the variability (standard deviation) among replicates. Below, we discuss the effects on each tensile property.

3.1 | Mechanical Properties

3.1.1 | Tensile Properties

Figure 4 illustrates the ultimate tensile strength (UTS) outcomes for material configurations A, B, and C with varied infill patterns. It is crucial to note that the UTS performance indicates that configuration B achieves a UTS of approximately 13.6 MPa with a Grid infill, exceeding that of configuration A (approximately 13 MPa).

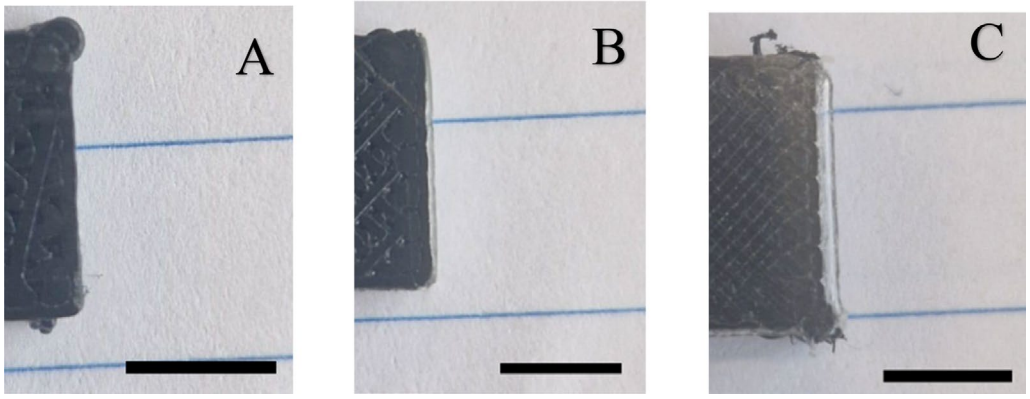

FIGURE 3 | (A) Print burring top right corner (B) Smaller print burring top right corner (C) Vertical view of specimen showcasing nylon displacement all taken on a leica DM2700M microscope at 5× magnification. [Color figure can be viewed at wileyonlinelibrary.com]

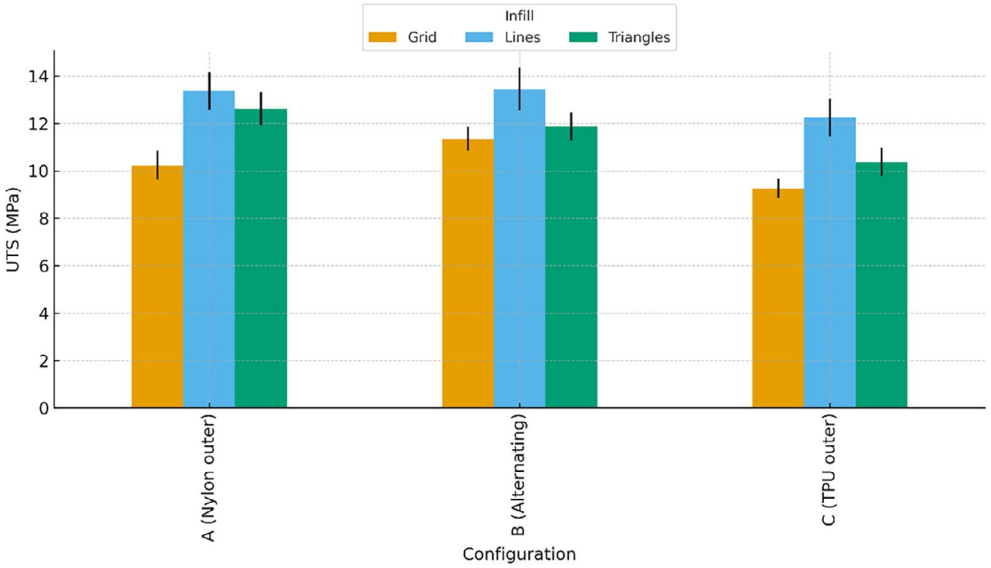

FIGURE 4 | Ultimate tensile strength (UTS) of TPU–Nylon composite specimens for each configuration. [Color figure can be viewed at wileyonlinelibrary.com]

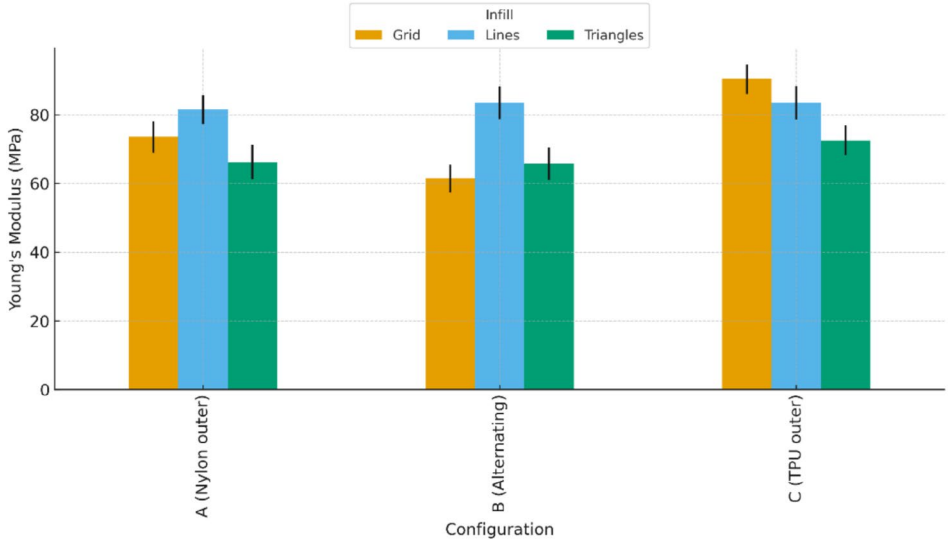

FIGURE 5 | Young's modulus of the TPU–Nylon specimens for each configuration and infill. [Color figure can be viewed at wileyonlinelibrary.com]

Variations in infill patterns also contribute to the UTS. The results demonstrate that the difference between the UTS values of the Grid and Lines infill patterns across configurations A and C approaches nearly 30%, while the disparity in UTS for configurations A versus C for the same infill pattern (e.g., Triangles) remains below 20% these findings suggest that alterations in the infill design can have comparable or greater impacts on UTS than changes in material configuration alone, consistent with literature by *A. liber*-Kneć and A. Łagan [24] that emphasizes the role that infill configurations play in tensile strength outcomes.

Unexpectedly, the highest UTS for the Grid infill is recorded under configuration B, deviating from conventional expectations where one would anticipate configuration B's performance to lie substantively between A and C. This anomaly may arise from complex interdependencies between mechanical properties and internal filament orientations. Configuration B facilitates more effective load distribution and stress resistance, thereby favoring tensile strength outcomes [25]. Research indicates that alternative infill patterns, such as those employed in configuration B, can reshape local stress responses and enhance overall structural integrity due to the preferential orientation of internal filaments and the geometrical arrangement of the infill [26, 27].

Figure 5 shows that stiffness trends do not exactly mirror those of strength. Notably, Configuration C (TPU outer) recorded the highest Young's modulus in one case (approximately 90 MPa, with a grid infill), even though C had the lowest UTS. This anomaly can be explained by the composition: the Nylon-rich core of configuration C provides initial rigidity under small

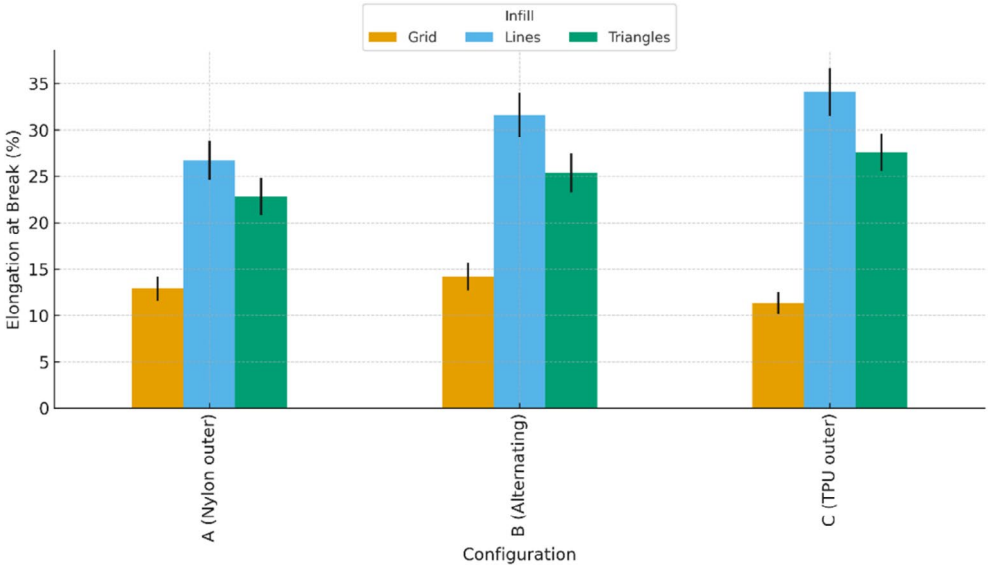

FIGURE 6 | Elongation at break of the TPU–Nylon specimens for each configuration and infill pattern. [Color figure can be viewed at wileyonlinelibrary.com]

tensile strains, temporarily raising the modulus, but the weak TPU shell still governs the ultimate failure (leading to low strength).

Meanwhile, configurations A and B exhibited moduli in the range of ~60–85 MPa. In terms of infill effects, the line pattern produced, on average, higher tensile moduli than either the grid or triangle patterns across all configurations. This is consistent with findings by S. Rajpurohit et al. and M. Hamoud et al. [28, 29] who reported that raster lines aligned with the loading direction (0° infill) yield stiffer, stronger tensile specimens than infill patterns with strands oriented transversely or at angles to the load. In our tests, the line infill oriented continuous polymer roads along the tension axis, maximizing the effective load-bearing area. By contrast, the grid and triangular infills introduced more interruptions (gaps) in the load direction, thereby reducing the effective cross-sectional area carrying the stress and lowering the observed modulus.

Figure 6 reveals a clear trade-off between strength and ductility. Configuration C (TPU outer) was the most ductile, reaching an elongation at break of approximately 34% strain (with a line infill), which is more than double the maximum elongation observed for configuration A. Configuration A (Nylon outer) was the most brittle, with elongation at break ranging from only about 12% up to 27% (the higher end achieved with a more compliant infill like the triangle pattern).

Configuration B (alternating layers) exhibited intermediate ductility, failing at approximately 25%–32% strain. These results demonstrate that incorporating more flexible TPU (especially in the outer layers, as in C) dramatically increases tensile elongation, albeit at the cost of strength. This behavior is consistent with the observations of K. Soltanmohammadi et al. [30], who found that adding TPU into a traditionally stiff thermoplastic (ABS) transformed the material response from brittle to highly extensible. In our case, the TPU-rich exterior in configuration C permits extensive deformation before fracture, whereas the stiff Nylon skins in configuration A restrict the overall strain at failure. Configuration B's layered structure allows it to achieve a compromise: it can sustain much higher strain than A while sacrificing only a small amount of strength relative to the optimal case.

Overall, tensile tests highlight distinct trade-offs among the three configurations. Configuration A provides the highest tensile strength and stiffness, but its ductility is limited. Configuration C delivers exceptional ductility but has significantly lower strength.

Configuration B offers a balance of properties, achieving near-maximum strength while retaining approximately 30% elongation. For applications requiring both high strength and high toughness, this alternating-layer design (B) appears to be the most effective. This finding aligns with the concept of functionally graded or sandwich composites reported in the literature. For example, S. Kumar et al. [4] observed that alternating stiff and soft layers in an FFF laminate helped distribute loads and accommodate deformation, thereby improving the combination of strength and ductility. Our results similarly suggest that judiciously arranging Nylon and TPU layers can achieve a synergistic balance between mechanical rigidity and flexibility.

Tensile testing revealed two dominant failure modes, as shown in Figure 7 in the dual-material FFF specimens: interlayer delamination and cohesive material rupture. Delamination was most prevalent in grid infill patterns and in the Nylon-outer configuration, where failure initiated along the TPU–Nylon interface. This behavior is consistent with previous studies showing that dissimilar polymer interfaces in multi-material FFF often exhibit limited molecular interdiffusion and low interfacial fracture toughness, particularly for Nylon–TPU systems [1]. In contrast, specimens printed with line infill and alternating TPU–Nylon layer arrangements predominantly failed by cohesive material rupture, exhibiting smooth stress–strain curves up to final

fracture, indicating effective load transfer across the interface. Aligned filament architectures are known to reduce interfacial peel stresses, while alternating-layer designs distribute interfacial stresses across multiple bonded regions, thereby delaying crack initiation and suppressing delamination [31]. Overall, the results demonstrate that material arrangement governs interfacial integrity, while infill geometry controls stress distribution and failure initiation, with line infill and alternating-layer configurations promoting cohesive failure and improved strength–ductility balance in dual-material FFF components.

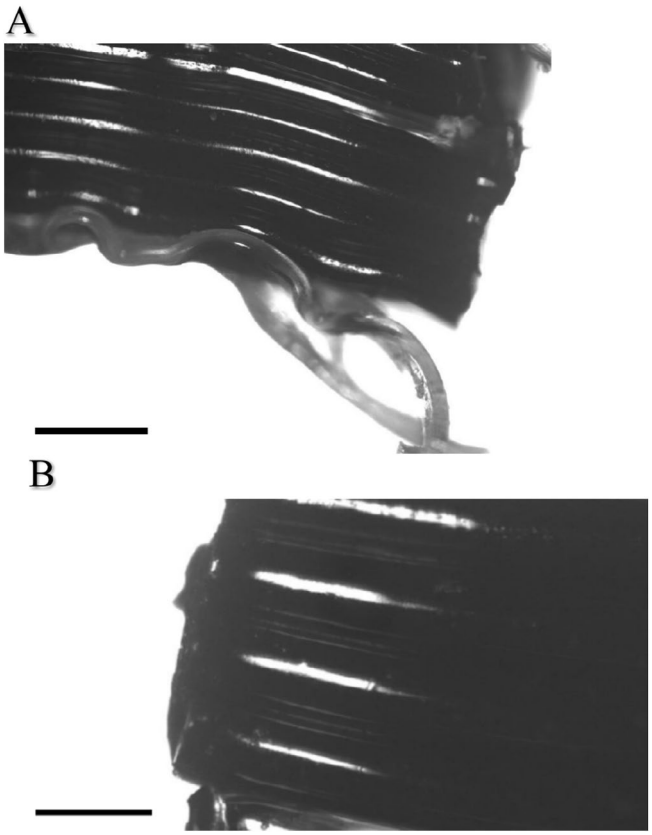

FIGURE 7 | (A) Fracture site—layer order A (B) Fracture site—layer order B (2 mm scale bar).

3.1.2 | Flexural Properties

Flexural testing (three-point bending) was performed to assess how the layer arrangement and infill geometry affect bending stiffness and strength. The flexural modulus and flexural strength of each specimen were measured, and Figures 8,9 summarize these results for the three configurations and various infill patterns (Lines, Grid, Triangles). Consistent with the tensile behavior, we find that the material configuration has the most pronounced impact on flexural performance, whereas the infill pattern plays a secondary role.

In bending, configuration A (Nylon outer) consistently exhibited the highest flexural stiffness and strength. For instance, with a triangular infill, configuration A achieved a flexural modulus of approximately 773 MPa and a flexural strength of approximately 74 MPa. These values are approximately 15%–20% higher than the best results obtained with either configuration B or C.

By contrast, configuration C (TPU outer) was the weakest in flexure, its modulus dropped to around 463 MPa and its strength to about 48 MPa in the worst case (observed with a grid infill). Configuration B (alternating layers) showed intermediate performance (e.g., ~659 MPa modulus and 66 MPa strength with a line infill), falling between A and C as expected. This ranking can be explained by the role of the outer skins in bending: under flexural load, the outer surfaces of the specimen carry the highest tensile and compressive stresses.

When the outer layers are Nylon (configuration A), Nylon's high stiffness resists bending, resulting in greater overall flexural rigidity and strength. Conversely, when the outer layers are soft TPU (configuration C), they deform more easily under stress,

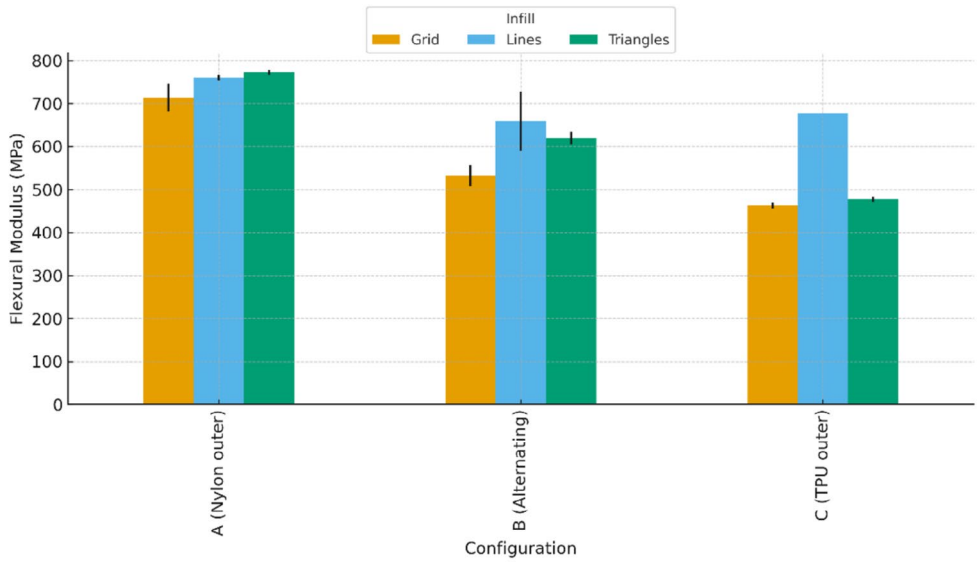

FIGURE 8 | Flexural modulus of the TPU–Nylon specimens for each configuration and infill. [Color figure can be viewed at wileyonlinelibrary.com]

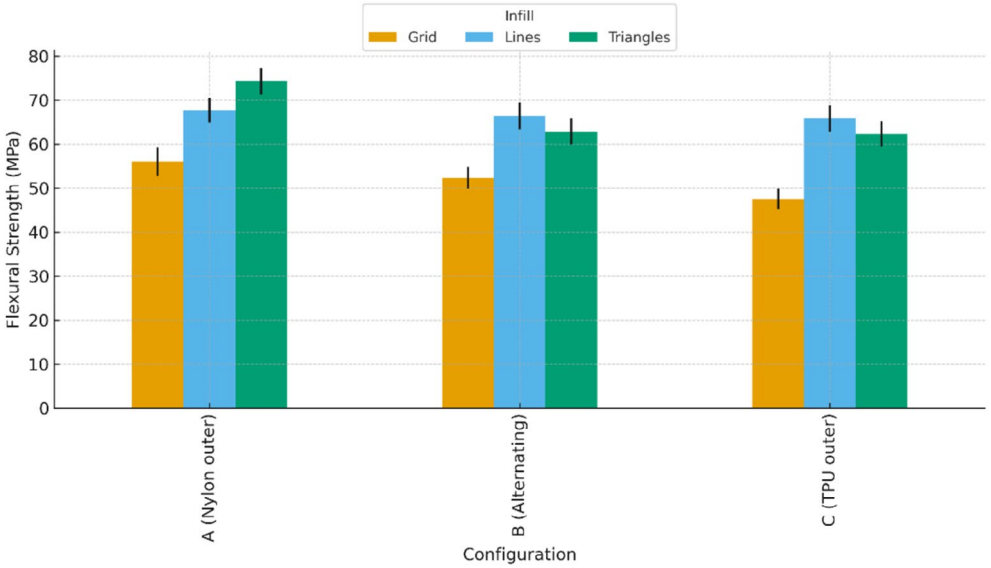

FIGURE 9 | Flexural strength of the TPU–Nylon specimens for each configuration and infill. [Color figure can be viewed at wileyonlinelibrary.com]

which diminishes the specimen's ability to carry load in bending. These results corroborate classic sandwich-structure theory and mirror the findings of A. Pinho and A. Piedade, M. Eryildiz [32, 33] who observed that in FFF-fabricated beams, the material used for the outer walls has a dominant influence on flexural stiffness and strength, outweighing the contribution of the infill in many cases.

The infill geometry had a measurable but secondary effect on flexural properties. In general, specimens with a Line infill outperformed those with a Grid infill in bending, especially for the less stiff configurations. For example, in configuration C (TPU outer), switching the infill from grid to lines increased the flexural strength from ~47.5 MPa to ~65.8 MPa and raised the flexural modulus from about 463 MPa to 677 MPa.

Configuration B showed a similar trend: using a line infill yielded roughly 20%–25% higher flexural metrics than using a grid infill (for instance, a strength of ~66 MPa with lines vs. ~52 MPa with grid). The Triangle infill pattern typically resulted in performance between these two extremes. Notably, in configuration A (Nylon outer), the triangle infill slightly outperformed the line infill in flexural strength (74 MPa vs. 68 MPa, respectively, as seen in Figure 9). This suggests that when the outer Nylon skins dominate the bending behavior, the infill pattern becomes less critical; any reasonably rigid infill will suffice to support the skins.

In configurations B and C, however, aligning more material along the primary stress direction (as the line pattern does along the beam's length) provides a clearer benefit. These observations are in line with the work of B. Arifvianto et al. V. Cojocaru et al. [34, 35] who noted that infill patterns oriented parallel to the loading direction can improve flexural performance by offering more continuous internal support, whereas patterns with orthogonal or angled strands (like grid) introduce more open channels and stress concentrations that can lead to earlier failure.

In summary, for flexural loading, configuration A is the optimal design among those tested, consistently yielding the highest modulus and strength across all infill patterns. Configuration B provides balanced bending performance but still falls short of configuration A, which achieves higher bending performance with its stiffer Nylon exterior. Configuration C remains the least effective for bending applications, although using a favorable infill (e.g., the line pattern) can partially mitigate these limitations. These findings provide practical insight for multi-material FFF design: if maximum bending stiffness and strength are required (as in structural or load-bearing components), a Nylon-outer configuration with an efficient infill is preferable. On the other hand, if some flexibility is desired, the alternating configuration B can be a good compromise, as it maintains much of the strength of configuration A while incorporating the TPU's toughness.

4 | Conclusion

This study demonstrated that dual-material fused filament fabrication (FFF) with thermoplastic polyurethane (TPU) and polyamide (Nylon) enables tunable mechanical performance by carefully controlling material configuration and infill geometry. The results showed that material arrangement has a more significant influence on mechanical behavior than infill pattern, with distinct performance trade-offs across the three tested configurations. The Nylon-outer configuration delivered the highest tensile and flexural strengths and exhibited superior stiffness, making it best suited for stiffness-critical structural components. The TPU-outer configuration displayed the greatest ductility, accommodating large strains with reduced strength, which is desirable for flexible or energy-absorbing elements. The alternating-layer configuration provided a balanced response, maintaining near-maximum strength while achieving substantial elongation, making it a versatile choice for multifunctional parts that must combine rigidity with deformation capacity.

Infill geometry also influenced performance, with line infill consistently outperforming grid and triangle patterns. Aligning extruded filaments with the loading direction improved stress transfer and reduced discontinuities, thereby enhancing both tensile and flexural responses. These results reinforce the understanding that FFF mechanical properties can be engineered through both macro-scale material placement and micro-scale deposition path design, providing a framework for tailoring hybrid material behavior.

From a practical perspective, the findings offer clear design and manufacturing guidelines. The Nylon-outer configuration is recommended for load bearing and housing components where stiffness is critical; the TPU-outer configuration for damping or compliant parts; and the alternating configuration for applications requiring a balance of strength and flexibility. The study also bridges design and process control by demonstrating that mechanical heterogeneity can be embedded directly during printing, reducing the need for post-assembly bonding or over molding.

Beyond its immediate engineering applications, the work has broader implications for research, education, and sustainable manufacturing. It provides an experimentally validated foundation for modeling and simulating dual-material systems, supporting the development of predictive design tools for additive manufacturing. In teaching, these insights can aid the integration of transitions between TPU and Nylon to improve interfacial continuity, explore performance under multi-axial and cyclic loading, and incorporate numerical simulation or in situ monitoring to optimize interlayer bonding. Overall, this study establishes a clear link between design architecture, processing strategy, and mechanical behavior in dual-material FFF, contributing to both theoretical understanding and practical adoption of hybrid additive manufacturing for high-performance and resource-efficient product development.

Author Contributions

Liam O'Connor: writing – original draft (lead), writing – review and editing (lead).

Acknowledgments

I want to acknowledge the contributions of Harley Collard and Eduardo Gonzalez in manufacturing the samples.

Funding

The author has nothing to report.

Conflicts of Interest

The author declares no conflicts of interest.

Data Availability Statement

The author has nothing to report.

References

1. C. G. Harris, N. J. S. Jursik, W. E. Rochefort, and T. W. Walker, "Additive Manufacturing With Soft TPU – Adhesion Strength in Multimaterial Flexible Joints," *Frontiers of Mechanical Engineering* 5 (2019): 00037, https://doi.org/10.3389/fmech.2019.00037.

2. L. O'Connor, "Comparative Analysis of the Mechanical Properties of FDM and SLA 3D Printed Components," *Journal of Micromanufacturing* (2025): 364689, https://doi.org/10.1177/25165984251364689.

3. L. O'Connor, "A Comparative Review of Material Supply Chains and Sustainability Pathways in Steel and Battery Technologies," *Extractive Industries and Society* 25 (2026): 101814, https://doi.org/10.1016/J.EXIS.2025.101814.

4. S. Kumar, I. Singh, S. S. R. Koloor, D. Kumar, and M. Y. Yahya, "On Laminated Object Manufactured FDM-Printed ABS/TPU Multimaterial Specimens: An Insight Into Mechanical and Morphological Characteristics," *Polymers (Basel)* 14 (2022): 4066, https://doi.org/10.3390/polym14194066.

5. S. Md, A. Nipu, T. Tang, et al., "Advances and Perspectives in Multi-Material Additive Manufacturing of Heterogenous Metal-Polymer Components," *Npj Advanced Manufacturing* 2, no. 1 (2025): 31, https://doi.org/10.1038/S44334-025-00045-W.

6. A. Giubilini and P. Minetola, "Multimaterial 3D Printing of Auxetic Jounce Bumpers for Automotive Suspensions," *Rapid Prototyping Journal* 29 (2023): 131–142, https://doi.org/10.1108/RPJ-02-2023-0066/FULL/PDF.

7. W. U. Usmani, F. P. Chietera, and L. Mescia, "Flexible Phased Antenna Arrays: A Review," *Sensors (Basel)* 25 (2025): 4690, https://doi.org/10.3390/S25154690.

8. R. M. Grzeskowiak, J. Schumacher, M. S. Dhar, D. P. Harper, P. Y. Mulon, and D. E. Anderson, "Bone and Cartilage Interfaces With Orthopedic Implants: A Literature Review," *Frontiers in Surgery* 7 (2020): 601244, https://doi.org/10.3389/fsurg.2020.601244.

9. B. J. Rashmi, C. Loux, and K. Prashantha, "Bio-Based Thermoplastic Polyurethane and Polyamide 11 Bioalloys With Excellent Shape Memory Behavior," *Journal of Applied Polymer Science* 134 (2017): 44794, https://doi.org/10.1002/app.44794.

10. Y. H. Que, Y. Shi, L. Z. Liu, et al., "The Crystallisation, Microphase Separation and Mechanical Properties of the Mixture of Ether-Based TPU With Different Ester-Based TPUs," *Polymers (Basel)* 13 (2021): 3475, https://doi.org/10.3390/POLYM13203475.

11. Q. F. Li, M. Tian, D. G. Kim, D. Z. Wu, and R. G. Jin, "Fracture and Impact Properties of Modified Nylon 11," *Journal of Applied Polymer Science* 83 (2002): 1600–1607, https://doi.org/10.1002/app.10154.

12. E. Brancewicz-Steinmetz, J. Sawicki, and P. Byczkowska, "The Influence of 3D Printing Parameters on Adhesion Between Polylactic Acid (PLA) and Thermoplastic Polyurethane (TPU)," *Materials (Basel)* 14 (2021): 6464, https://doi.org/10.3390/MA14216464.

13. J. S. Song and Y. Zhang, "Predictive Three-Dimensional Printing of Spare Parts With Internet of Things," 71 (2024): 1925–1943, https://doi.org/10.1287/MNSC.2023.00978.

14. S. Turaka, V. Jagannati, B. Pappula, and S. Makgato, "Impact of Infill Density on Morphology and Mechanical Properties of 3D Printed ABS/CF-ABS Composites Using Design of Experiments," *Heliyon* 10 (2024): e29920, https://doi.org/10.1016/j.heliyon.2024.e29920.

15. N. Vidakis, M. Petousis, A. Korlos, et al., "Strain Rate Sensitivity of Polycarbonate and Thermoplastic Polyurethane for Various 3D Printing Temperatures and Layer Heights," *Polymers* 13 (2021): 2752, https://doi.org/10.3390/POLYM13162752.

16. M. Sardinha, L. Ferreira, H. Diogo, T. R. P. Ramos, L. Reis, and M. F. Vaz, "Material Extrusion of TPU: Thermal Characterization and Effects of Infill and Extrusion Temperature on Voids, Tensile Strength and Compressive Properties," *Rapid Prototyping Journal* 31 (2024): 62–81, https://doi.org/10.1108/RPJ-06-2024-0241/FULL/PDF.

17. A. Yankin, Y. Alipov, A. Temirgali, et al., "Optimization of Printing Parameters to Enhance Tensile Properties of ABS and Nylon Produced

by Fused Filament Fabrication," *Polymers* 15 (2023): 3043, https://doi.org/10.3390/POLYM15143043.

18. J. Slapnik, R. Lorber, I. Pulko, M. Huskić, and K. P. Črešnar, "Overprinting of TPU Onto PA6 Substrates: The Influences of the Interfacial Area, Surface Roughness and Processing Parameters on the Adhesion Between Components," *Polymers* 16 (2024): 650, https://doi.org/10.3390/POLYM16050650.

19. A. S. Karad, P. D. Sonawwanay, M. Naik, and D. G. Thakur, "Experimental Study of Effect of Infill Density on Tensile and Flexural Strength of 3D Printed Parts," *Journal of Engineering and Applied Science* 70 (2023): 1–17, https://doi.org/10.1186/S44147-023-00273-X/FIGURES/15.

20. S. Dağlı, "Mechanical Characterization and Interface Evaluation of Multi-Material Composites Manufactured by Hybrid Fused Deposition Modeling (HFDM)," *Polymers* 17 (2025): 1631, https://doi.org/10.3390/POLYM17121631.

21. I. S. ELDeeb, E. Esmael, S. Ebied, et al., "Optimization of Nozzle Diameter and Printing Speed for Enhanced Tensile Performance of FFF 3D-Printed ABS and PLA," *Journal of Manufacturing and Materials Processing* 9 (2025): 221, https://doi.org/10.3390/JMMP9070221.

22. J. S. Ramírez-Prieto, J. S. Martínez-Yáñez, and A. G. González-Hernández, "Effect of Raster Angle on the Tensile and Flexural Strength of 3D Printed PLA+ Parts," *AIMS Materials Science* 12 (2025): 363–379, https://doi.org/10.3934/matersci.2025019.

23. X. Wang, S.-C. Li, D.-W. Xiang, et al., "Flexural Properties and Failure Mechanisms of Short-Carbon-Fiber-Reinforced Polylactic Acid Composite Modified With MXene and GO," *Materials* 17 (2024): 1389, https://doi.org/10.3390/MA17061389.

24. A. Liber-Kneć and S. Łagan, "Effect of Mass Reduction of 3D-Printed PLA on Load Transfer Capacity—A Circular Economy Perspective," *Materials* 18 (2025): 3262, https://doi.org/10.3390/MA18143262.

25. S. Ganeshkumar, S. D. Kumar, U. Magarajan, et al., "Investigation of Tensile Properties of Different Infill Pattern Structures of 3D-Printed PLA Polymers: Analysis and Validation Using Finite Element Analysis in ANSYS," *Materials* 15, no. 15 (2022): 5142, https://doi.org/10.3390/MA15155142.

26. L. K. Guo, L. B. Chen, Z. W. Chen, and J. Y. Wang, "Enhancing UHPC Tensile Performance Using Polystyrene Beads: Significant Improvements and Mechanisms," *Materials* 17 (2024): 2479, https://doi.org/10.3390/MA17112479.

27. P. Chansamai, T. Seangpong, and V. Uthaisangsuk, "Effect of Raster and Layer Characteristics on Tensile Behavior and Failure of FFF Printed PLA Samples by Representative Volume Element Model," *Proceedings of the Institution of Mechanical Engineers, Part B: Journal of Engineering Manufacture* 238 (2024): 1463–1473, https://doi.org/10.1177/09544054231202210.

28. M. Hamoud, A. B. Elshalakany, M. Gamil, and H. Mohamed, "Investigating the Influence of 3D Printing Parameters on the Mechanical Characteristics of FDM Fabricated (PLA/cu) Composite Material," *International Journal of Advanced Manufacturing Technology* 134 (2024): 3769–3785, https://doi.org/10.1007/s00170-024-14313-0.

29. S. R. Rajpurohit, H. K. Dave, and K. P. Rajurkar, "Prediction of Tensile Strength of Fused Deposition Modeling (FDM) Printed PLA Using Classic Laminate Theory," *Engineering Solid Mechanics* 10 (2022): 13–24, https://doi.org/10.5267/j.esm.2021.12.002.

30. K. Soltanmohammadi, D. Rahmatabadi, M. Aberoumand, et al., "Effects of TPU on the Mechanical Properties, Fracture Toughness, Morphology, and Thermal Analysis of 3D-Printed ABS-TPU Blends by FDM," *Journal of Vinyl and Additive Technology* 30 (2024): 958–968, https://doi.org/10.1002/vnl.22097.

31. Q. Sun, S. T. Potu, J. Man, et al., "Effect of Infill Pattern on the Mechanical Properties and Stress Relaxation Behavior of 3D Printed PEEK," *Journal of Materials Research and Technology* 39 (2025): 5306–5318, https://doi.org/10.1016/J.JMRT.2025.10.170.

32. A. C. Pinho and A. P. Piedade, "Sandwich Multi-Material 3D-Printed Polymers: Influence of Aging on the Impact and Flexure Resistances," *Polymers* 13 (2021): 4030, https://doi.org/10.3390/POLYM13224030.

33. M. Eryildiz, "Comparison of Maximum Number of Walls and 100% Infill Density Parameters on Flexural Strength to Obtain FDM Build 3D Solid Parts," *Engineering and Applied Natural Sciences* 1 (2022): 334–338.

34. V. Cojocaru, D. Frunzaverde, and C. O. Miclosina, "On the Behavior of Honeycomb, Grid and Triangular PLA Structures Under Symmetric and Asymmetric Bending," *Micromachines* 14 (2023): 120, https://doi.org/10.3390/MI14010120.

35. B. Arifvianto, B. E. Satiti, U. A. Salim, I. Suyitno, A. Nuryanti, and M. Mahardika, "Mechanical Properties of the FFF Sandwich-Structured Parts Made of PLA/TPU Multi-Material," *Progress in Additive Manufacturing* 7 (2022): 1213–1223, https://doi.org/10.1007/S40964-022-00295-6.